

## Effects of some additives on the corrosion behaviour and preferred orientations of zinc obtained by continuous current deposition

M. MOUANGA<sup>1</sup>, L. RICQ<sup>1</sup>, J. DOUGLADE<sup>2</sup> and P. BERÇOT<sup>1,\*</sup>

<sup>1</sup>Laboratoire de Chimie de Matériaux et Interfaces, Université de Franche-Comté, 16 route de Gray, 25030, Besançon Cedex, France

<sup>2</sup>D.T.I., E.A.3083, Université de Reims, B.P. 1039, 51687, Reims Cedex, France

(\*author for correspondence, tel.: +33-3-81-66-20-30, e-mail: patrice.bercot@univ-fcomte.fr)

Received 8 September 2005; accepted in revised form 6 October 2006

**Key words:** zinc, electrodeposition, additives, corrosion, x-ray Diffraction, scanning electron microscopy

### Abstract

The effect of thiourea, urea and guanidin on zinc deposits obtained from chloride baths under continuous current conditions are described and discussed. The corrosion behaviour of the deposits was investigated in an aerated 3.5% NaCl solution; anodic polarization curves, polarization resistance ( $R_p$ ) measurements and weight-loss studies were performed. The corrosion resistance of zinc deposits improved in the presence of urea. The deposit morphology was analyzed using Scanning Electron Microscopy (SEM) and X-Ray Diffraction (XRD) was used to determine the preferred crystallographic orientations of the deposits. The preferred crystallographic orientations of zinc deposits (112) do not change in the presence of urea and guanidin except for an increase in the peak intensity of the (112) plane. In the presence of thiourea, zinc deposits crystallise in two textures; (100) and (110). The influence of each additive and the difference between additives on the zinc deposits are also discussed.

### 1. Introduction

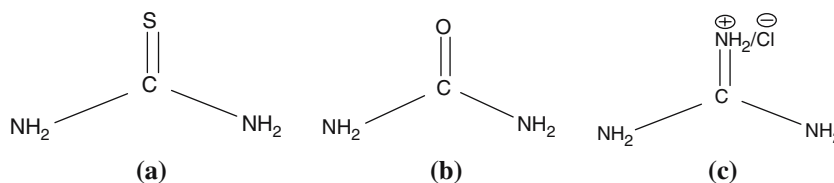
Zinc deposits are essentially used to protect steel against corrosion [1]. The potential of zinc deposits is more negative (−1050 mV/SCE) than that of steel (−650 mV/SCE) under the same conditions (3.5% NaCl solution). Thus, zinc deposits behave as sacrificial anodes and offer cathodic protection. It is well known that additives which are often organic compounds are added to improve zinc deposit properties. Organic compounds containing oxygen, sulphur and nitrogen are among the most widely used as corrosion inhibitors of zinc in electroplating [2–10]. These compounds can adsorb on the zinc surface with an impact on deposit properties and the electroplating process. The incorporation of sulphur has several effects such as lowering corrosion resistance, as reported in the case of bright nickel electrodeposits [11]. However, no study has been reported (to our knowledge) on the additives with the same structure (with only one atom difference) by comparison of their effects on electroplated zinc. The sulphur atom in thiourea is replaced by the oxygen atom in urea and by the  $\text{NH}_2^+/\text{Cl}^-$  group in guanidin (Scheme1). The use of these additives allows us to compare the effect of sulphur, nitrogen and oxygen on the corrosion behaviour, morphology and preferred orientations of the deposits. In this study the deposits

were obtained at room temperature using continuous current without stirring.

### 2. Experimental

Zinc samples were prepared by electrodeposition on the DC 01 panel steel from chloride baths at room temperature and without stirring (Table 1). The electrolytes were prepared using milli-Q water. The thickness of electrodeposits was  $13 \pm 1 \mu\text{m}$  and the deposits area was (2 cm × 2 cm). Prior to each electrodeposition, the tested steels were degreased in sodium hydroxide solution (40 g L<sup>−1</sup>; 64.5 °C), then mechanically cleaned with emery paper (1000) and etched with hydrochloric acid solution (pH = 0.5) for two minutes and rinsed with distilled water.

A scanning electron microscope (JSM-5600) was used to analyze the morphology of the deposits obtained under various conditions. The preferred orientations of the deposits were determined by an XRD using a D8 advance Bruker (with Bragg–Bretano configuration) with Cu-K $\alpha$  radiation ( $\lambda = 1.54 \text{ \AA}$ ). The  $2\theta$  range of 30° to 100° was recorded at a rate of 0.02° s<sup>−1</sup>. The texture coefficients ( $T_c$ ) of the zinc deposits were calculated from the X-ray data using the Bruker program.



Scheme 1. Structures of additives, (a) thiourea, (b) urea, (c) guanidin.

Table 1. Plating bath composition for zinc electrodeposition

Solution compositions
65 g L <sup>-1</sup> ZnCl <sub>2</sub> + 200 g L <sup>-1</sup> KCl + 20 g L <sup>-1</sup> H <sub>3</sub> BO <sub>3</sub> (basic solution)
basic solution + 13 × 10 <sup>-3</sup> mol L <sup>-1</sup> urea
basic solution + 13 × 10 <sup>-3</sup> mol L <sup>-1</sup> guanidin
basic solution + 13 × 10 <sup>-3</sup> mol L <sup>-1</sup> thiourea

The thickness of the deposits was determined by a high Performance energy dispersive X-ray fluorescence measuring instrument (EDXRF) using a Fischerscope X-Ray XDAL.

Anodic polarization was carried out in 3.5% NaCl solution. A three-electrode cell was used. The working electrode (WE) was masked with lacquer to expose a 1 × 1 cm<sup>2</sup> area. Platinum wire was used as the counter electrode (CE) with a saturated calomel electrode (SCE) as a reference electrode.

The WE was kept in the 3.5% NaCl electrolyte for 40 min to establish the potential. The WE was then polarized from the open circuit potential (OCP) against SCE to 200 mV at a scan rate of 30 mV min<sup>-1</sup>.

The polarization resistance ( $R_p$ ) was measured on eight days during immersion. For each plating bath, 28 samples of zinc deposits were weighed ( $m_i$ ), the index  $i$  refers to the zinc deposit samples. The WE was masked with lacquer to expose a 1.5 × 1.5 cm<sup>2</sup> area. A three-electrode cell was also used.

The linear polarization resistance experiments were performed using a scan rate of 0.1 mV s<sup>-1</sup> in order to determine the values of  $R_p$  on different days. These experiments were carried out by scanning the potential from -7 to +3 ± 0.5 mV (vs. E<sub>corr</sub>).

The average value of the polarization resistance ( $R_p$ ) measurements was determined from the slope of the current-potential line in the range of ±2 mV about the corrosion potential [12].

$$R_p = \left( \frac{d\eta}{di} \right)_{i \rightarrow 0} \quad (1)$$

According to Rochaix [13]:

$$I_{corr} = \frac{RT}{nFR_p} \quad (2)$$

i.e. the higher the polarization resistance the better the corrosion resistance.

In order to study the weight-loss, after polarization resistance measurements were taken for all zinc deposits; four samples were removed, dried and weighed ( $m'_i$ ) each

day from the second day to the eighth day. The weight-loss ( $\Delta m$ ) was calculated as  $\Delta m = (m_i - m'_i)$  and after being removed and weighed, the four samples were not used again.

### 3. Results and discussion

#### 3.1. Morphology and texture of zinc deposits

The zinc electrocrystallization process is very sensitive to bath composition, so it was of interest to determine the texture of all the investigated Zn deposits. The preferred orientations of the deposits were determined using Muresan's method [14–17] calculating the texture coefficient ( $T_c$ ) with the equation:

$$T_c(hkl) = \frac{I(hkl)}{\sum I(hkl)} \times \frac{\sum I_0(hkl)}{I_0(hkl)} \times 100 \quad (3)$$

where  $I(hkl)$  is the peak intensity of the zinc electrodeposits and  $\sum I$ , is the sum of the intensities of the independent peaks. The index 0 refers to the intensities for the standard zinc powder sample. The preferred crystallographic orientation is indicated by a  $T_c$  value larger than unity. The diffractograms are shown in Figure 1 and texture coefficients are given in Table 2. From the data in Table 2, it is clear that in the absence of additives, 46.5% of zinc sample crystallites were oriented parallel to the pyramidal (112) plane and 18.1% were parallel to the prismatic (110) plane. The pyramidal (112) is the preferred crystallographic orientation for zinc deposits in the absence of additives. Filho et al. [18] have reported that at a high current density, the diffracted intensities of the (002)<sub>Zn</sub>, (105)<sub>Zn</sub> and (104)<sub>Zn</sub> crystallographic planes decrease and the diffracted intensities of the (101)<sub>Zn</sub> and (112)<sub>Zn</sub> crystallographic planes increase. The diffracted intensities of (100)<sub>Zn</sub> and (110)<sub>Zn</sub> are the only crystallographic planes which appeared at high current density. The obtained (112) crystallographic orientation of zinc deposits in the absence of additives at  $J = 4 \text{ A dm}^{-2}$  is in agreement with the literature. In the presence of urea, 57.6% of zinc deposits crystallize along the (112) plane and 49.5% of the deposits show the same trend in the presence of guanidin. In the presence of thiourea, zinc deposits crystallize into two textures (100) at 31.6% and (110) at 28.0%.

As the additives are added to the solution, they are adsorbed on the electrode, which affects the reduction of metal ions and modifies the crystallographic

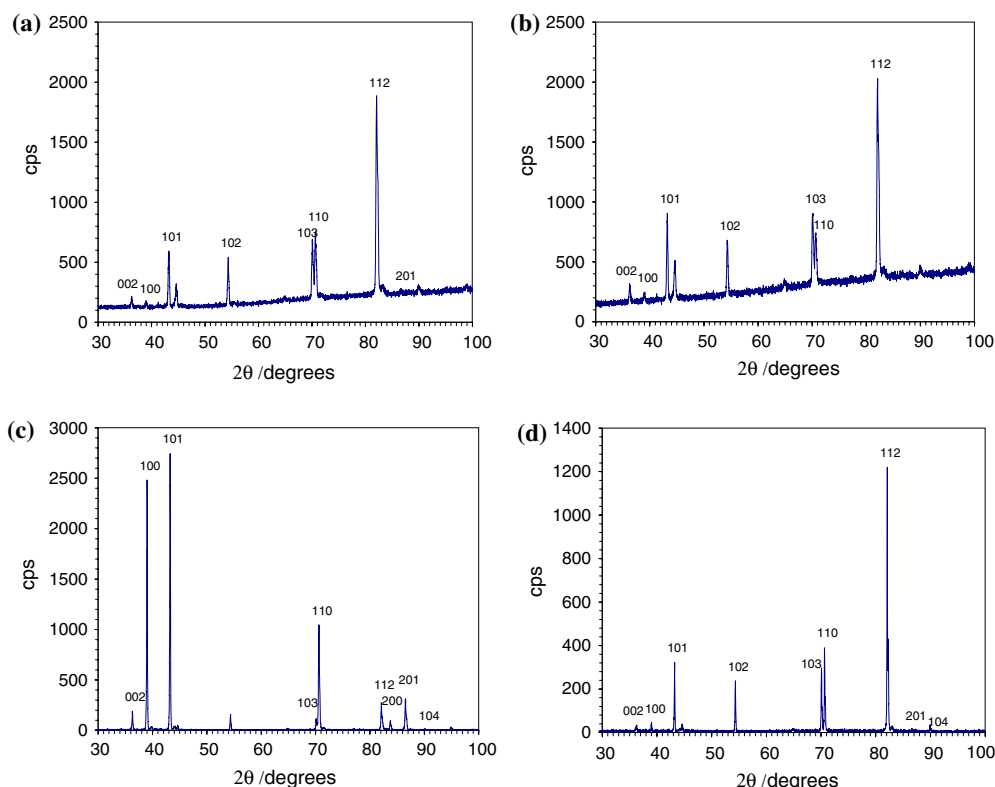


Fig. 1. X-ray diffractograms of electrodeposited zinc (a) without additive, (b) with guanidin, (c) with thiourea, (d) with urea.

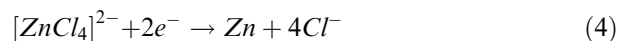
Table 2. Texture coefficients ( $T_c$ ) of Zn deposits

Plane ( $hkl$ )	$T_c$ ( $hkl$ ) (%) for electrodeposit systems			
	Basic solution	Urea	Guanidin	Thiourea
002	0.7	0.41	1.3	1.45
100	0.8	0.9	1.2	31.61
101	1.5	1.8	2.8	8.04
102	9.1	8.85	11.5	3
103	10	9.68	14.9	1.93
110	18.1	19.69	16.3	27.83
004	0	0	0	1.85
112	46.5	57.57	49.5	6.6
200	0	0	0	1.93
201	1.5	1.1	2.4	11.34
104	11.8	0	0	4.42

orientations of the deposits. Thus, a voltammetric study was carried out to complete the investigation of the additive effects. Figure 2 shows the  $j$  versus  $E$  curves obtained for the Zn(II) solution in the presence and absence of additives at a scan rate of  $50 \text{ mV min}^{-1}$ . For comparison, linear voltammograms obtained in the same conditions without Zn(II) in the solution are presented in Figure 3. The presence of additives shifts the potential toward more negative values.

In a more negative potential region (Figure 2), the reduction of Zn(II) ions occurs. The mechanism of Zn(II) ion reduction from a chloride bath was proposed by Trejo et al. [19, 20] and supported by Rojas et al. [21, 22]. They have reported that the chloride ions ( $\text{Cl}^-$ )

establish a complex with zinc ions and this complex is reduced to zinc as follows:



The potential at which the reduction occurs can be calculated from the following equation:

$$E_{\text{ZnCl}_4^{2-}/\text{Zn}} = -1.01 + 0.12p\text{Cl} - 0.03p\text{Zn} \quad (5)$$

As expected, the additives affect the zinc electrodeposition process (Figure 2). The negative shift of potential at  $J = 4 \text{ A dm}^{-2}$  increases in the following

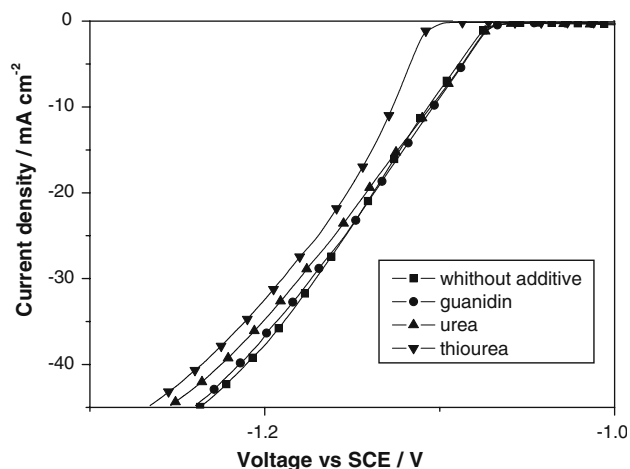


Fig. 2. Cathodic polarization curves obtained on panel steel from plating bath without stirring.

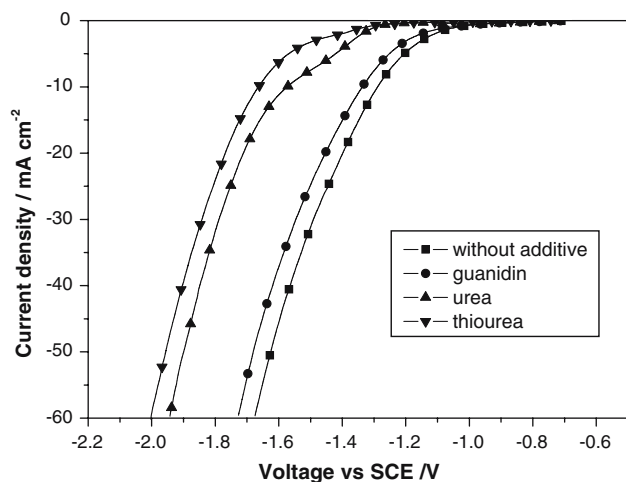


Fig. 3. Cathodic polarization curves obtained on panel steel from plating bath without Zn(II) ions and without stirring.

order: guanidin, urea and thiourea. An increase in the metal deposition potential has been observed in the presence of additives [23–26]. This result is usually interpreted in terms of partial coverage of the electrode surface by the additive. This blocks the active sites, decreasing the nucleation rate and affecting the nucleation mechanism [27]. In addition, adsorption of the additive molecules on the growing zinc deposit can occur, blocking the electrocrystallization process, as observed by Gomes et al. who studied surfactant effects on zinc electrodeposits [28]. Consequently, metallic deposits obtained in the presence of additives have a smaller grain size. The inhibition depends on the structure, size of the additives and the specific interactions between the additive and the substrate as well as the additive and the deposit. Reents et al. [29] studied the influence of thiourea on silver deposition and reported that thiourea adsorbs onto the substrate and deposit through the sulphur atom.

Considering the structure of thiourea and urea, thiourea adsorbs onto the zinc deposits through the sulphur atom and urea adsorbs through the oxygen atom. The same effect of thiourea and urea on the potential shift is expected. The difference observed, can be attributed to the fact that the sulphur atom in thiourea has more electrons than the oxygen atom in urea; thiourea is more disposed to interact with the substrate or the zinc deposits. The nitrogen atom in guanidin does not possess free electrons, thus there is no interaction between guanidin molecules and the substrate or the zinc deposits.

The difference in the crystallographic orientations between thiourea (100) and (110) and guanidin (112) or urea (112) is attributable to the sulphur atom. The oxygen atom (urea) and nitrogen atom (guanidin) produced zinc deposits with the same crystallographic orientations (112).

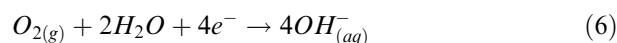
Some structural differences between the investigated zinc deposits can also be detected from morphological studies. Figure 4 shows the SEM micrographs of zinc

deposits. All electrodeposits appear sufficiently well distributed, compact and continuous. The use of guanidin does not refine the grain size of the deposits, whereas zinc deposits with smaller grain size are obtained in the presence of thiourea compared to those obtained in the absence of additives.

### 3.2. Corrosion behaviour

Several studies concerning the corrosion behaviour of zinc in NaCl solutions have been carried out, where the corrosion of zinc proceeds via two partial reactions.

- (i) The cathodic reaction is the reduction of oxygen and leads to a pH increase [30]



- (ii) The anodic reaction involves the dissolution of zinc and leads to weight loss [31, 32]



The anodic polarization of pure zinc was conducted to better understand the corrosion behaviour of deposits in 3.5% NaCl solution. A typical anodic polarization curve for pure zinc is shown in Figure 5. This curve has two regions. The first consists of active dissolution (from  $E_{corr}$  to point a) of zinc and zinc dissolution continues with increasing potential until zinc hydroxy-chloride (ZHC) forms and covers the surface (point a). Many authors have reported that ZHC forms on the surface of the zinc deposits during exposure to NaCl solution [30, 31, 33]. Zhang [34] has reported that the ZHC layer formed in NaCl solution at  $pH < 7$  (acidic media) is porous. With this observation, the ZHC layer can be classified as a pseudo-passive layer [35]. From point a, the pseudo-passive layer (ZHC) forms on the zinc surface and the zinc dissolution continues, but the rate decreases [36].

When metal passivation occurs, the current density drops, as the potential increases [13]. Although there is an increase in potential, shown in Figure 5, the current density does not drop. Geary et al. [32] have also observed the same behaviour of pure zinc in a  $0.5 \text{ mol dm}^{-3}$  NaCl solution. It is evident that in an acidic NaCl solution a passive layer does not form, but it forms a zinc hydroxy-chloride, which is a pseudo-passive layer. When the whole sample surface is covered by this layer the rate of zinc dissolution decreases.

The anodic polarization curves shown in Figure 6 do not exhibit Tafel behaviour. In the presence of thiourea the zinc deposit curve is near to a free zinc curve. Although a finer grain size is obtained in the presence of thiourea, as well as a different crystallographic orientation, the use of thiourea does not improve the corrosion resistance of zinc deposits. Kumar et al. [37] also used thiourea from chloride media. They reported the non-improvement of corrosion resistance of the zinc deposits in the presence of thiourea. The corrosion behaviour of

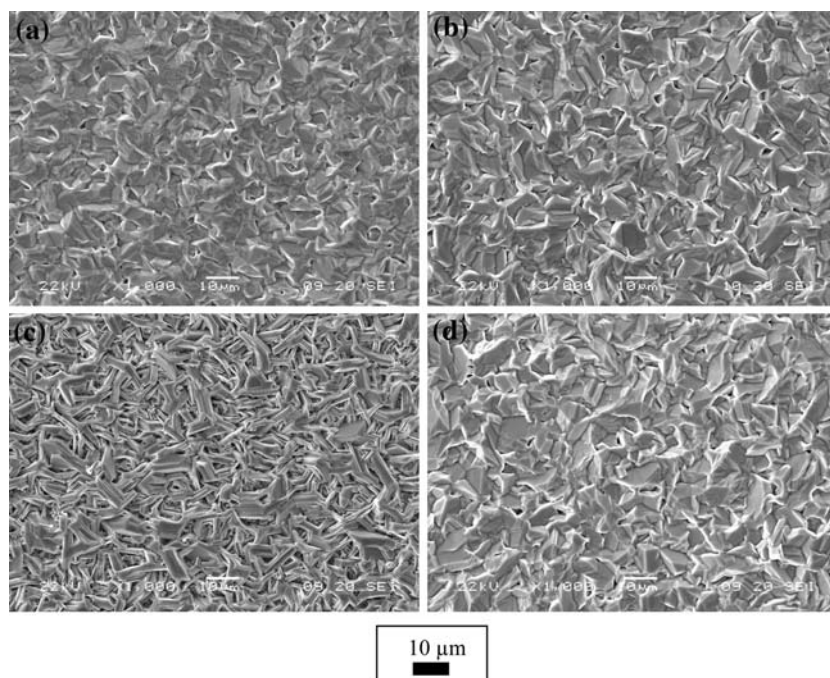


Fig. 4. SEM micrographs of zinc deposits (a) zinc without additive, (b) zinc with guanidin, (c) zinc with thiourea, (d) zinc with urea.

metallic coatings is dependent on the texture, morphology and chemical composition of the deposits [38]. Sulphur is incorporated into the deposits in the presence of thiourea [39]. It is well known that the presence of a sulphur atom in the deposits decreases the corrosion resistance, as reported for bright nickel electrodeposits [11]. In contrast, in the presence of thiourea, the deposits have a finer grain size. The finer grain size of the zinc coatings improves the corrosion resistance [39]. In spite of the thiourea effects on morphology and texture, thiourea does it not.

The anodic polarization curves of zinc deposits obtained in the presence of guanidin are also close to those of free zinc. The use of this additive does not improve the corrosion resistance. The morphology and texture of the deposits obtained in the presence of

guanidin are also similar to those in the absence of additives. Thus, the corrosion behaviour of zinc deposits obtained in the presence of guanidin is the same as that obtained in the absence of additives.

The anodic polarization curves of zinc deposits obtained in the presence of urea are under those obtained in the absence of additives. The corrosion resistance is improved by adding urea to the bath. The deposit texture in the presence of urea is the same as that obtained in the absence of additives, while the intensity of the (112) plane is increased in the presence of urea. When a metal is exposed to a corrosive environment the corrosion rate of each grain varies due to the difference in the binding energy of atoms between the crystallographic planes [38]. In the presence of urea, the peak

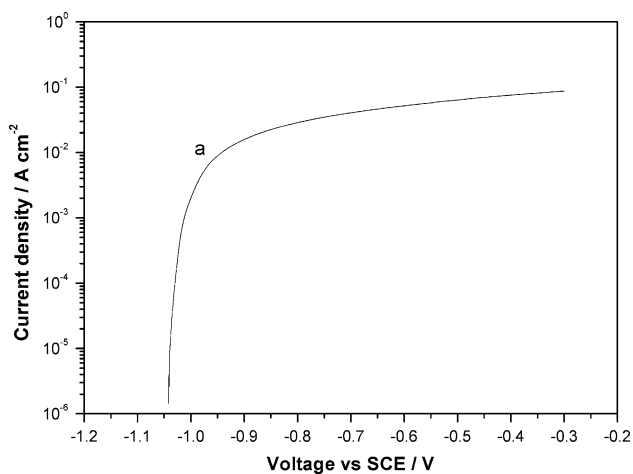


Fig. 5. Polarization curve for pure zinc in 3.5% NaCl solution.

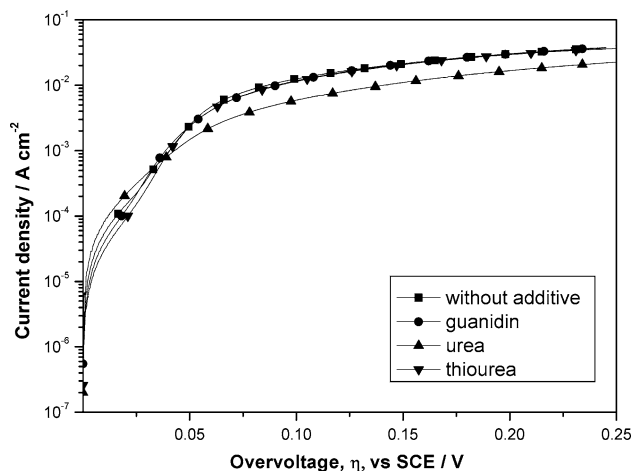


Fig. 6. Anodic polarization curves for Zn deposits in a 3.5% NaCl solution: with and without additive.

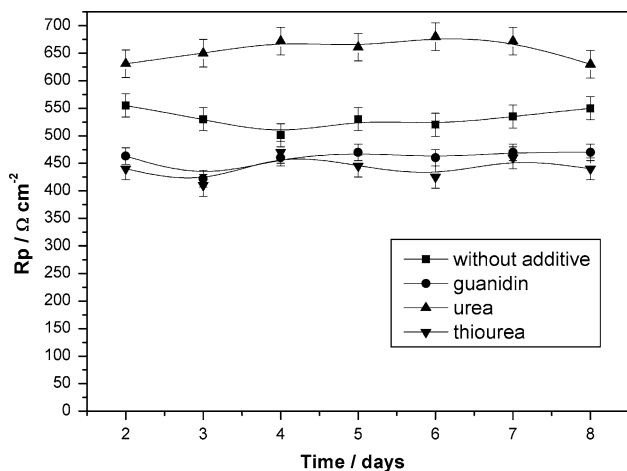


Fig. 7. Polarization resistance curves of zinc deposits: with and without additive.

intensity of the (112) crystallographic plane increases. The increase in texture intensity can improve the corrosion resistance of the coatings as observed by Park et al. from the (001) plane [38]. From the cathodic polarization data (Figure 2), in the presence of urea, the zinc deposits have a slightly finer grain size.

In order to confirm the anodic polarization results, other corrosion tests were carried out (polarization resistance and weight-loss studies). Figure 7 shows the polarization resistance ( $R_p$ ) curves and Figure 8 shows the weight-loss curves. The polarization resistance remains constant during the eight days of exposure to the NaCl solution. No difference is observed between the zinc deposits obtained in the presence of thiourea, guanidin and the zinc deposits obtained in the absence of additives, while in the presence of urea, the  $R_p$  curve is higher than that of free zinc. The corrosion resistance of zinc deposits is improved in the presence of urea. The  $R_p$  results are in agreement with those obtained by the anodic polarization method. The polarization resistance measurements were carried out in parallel with the

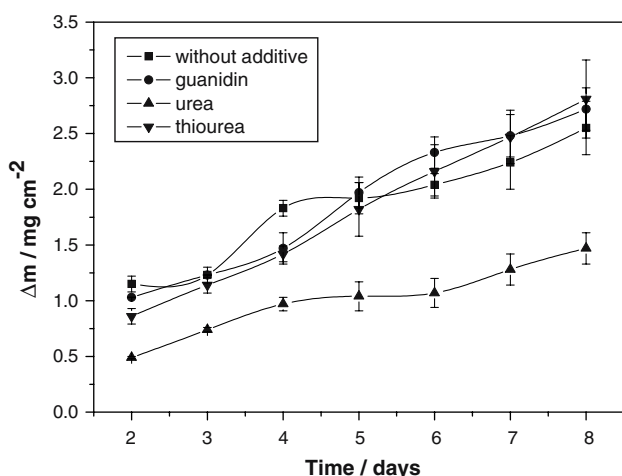


Fig. 8. Weight-loss curves of zinc deposits: without additive, with guanidin, with thiourea, with urea.

weight-loss ones. Figure 8 shows the weight-loss curves of deposits obtained in the presence and absence of additives. A lower weight-loss rate is observed with the deposits obtained in the presence of urea.

All these curves confirm the improvement in corrosion resistance of the deposits in the presence of urea and the non-improvement of the corrosion behaviour in the presence of thiourea or guanidin.

#### 4. Conclusion

In this study, zinc deposits with a finer grain size were obtained in the presence of thiourea, while guanidin had no significant effect on the morphology compared to that obtained in the absence of additives. The crystallographic orientation of the zinc deposits changes from (112) in the absence of additives to a pseudo texture (100) and (110) in the presence of thiourea. Guanidin and urea have the same crystallographic orientation with the deposits obtained in the absence of additives, but in the presence of these additives, the peak intensity of the (112) plane increases. The use of thiourea or guanidin does not improve the corrosion resistance of the deposits while an improvement in corrosion resistance was observed with urea.

The difference in the effects between thiourea, urea and guanidin is attributable to the molecular structures of the additives.

#### Acknowledgement

The authors thank Lindsay Myers for corrections to this paper.

#### References

1. L. Lacourcelle, 'Traité de galvanotechnique' (Galva-conseil, 1997) p. 234.
2. C.S. Venkatachalam, S.R. Rajagopalan and M.V.C. Sastry, *Electrochim. Acta* **26** (1981) 1257.
3. M. Troquet and J. Pegeiti, *Electrochim. Acta* **27** (1982) 197.
4. A.S. Fouda, A.H. Elasklary and L.H.M. Maadkeur, *J. Ind. Chem. Soc.* **59** (1984) 425.
5. C.A. Witt, I. Drziszga and W. Kola, *Metall* **39** (1985) 828.
6. L. Horner and E. Pliefke, *Werkst. Korros.* **37** (1986) 457.
7. A.I. Ahmed and S.A. Hakam, *Anti-corrosion* **3** (1989) 4.
8. K. Wipperman, J.W. Shultze, R. Kessel and J. Penninger, *Corros. Sci.* **32** (1991) 205.
9. M.S.A. Aal, Z.A. Ahmed and M.S. Hassan, *J. Appl. Electrochem.* **22** (1992) 1104.
10. E.E.F. Sherbini, S.M.A. Wahaab and M. Deyab, *Mater. Chem. Phys.* **89** (2005) 183.
11. M. Schlesinger and Paunovic M. 'Modern electroplating' (John Wiley and Sons, Inc., 2000) p. 151.
12. K.M.S. Youssef, C.C. Koch and P.S. Fedkiw, *Corros. Sci.* **46** (2004) 51.
13. C. Rochaix, *Electrochimie, thermodynamique-cinétique*, Nathan (1996) p. 120.

14. L. Muresan, L. Oniciu, M. Froment and G. Maurin, *Electrochim. Acta* **37** (1992) 2249.
15. P. Fricoteaux and J. Douglade, *J. Mater. Sci. Lett.* **21** (2002) 1485.
16. S.H. Kim, H.J. Sohn, Y.C. Joo, Y.W. Kim, T.H. Yim, H.Y. Lee and T. Kang, *Surf. Coat. Technol.* **199** (2005) 43.
17. R. Ramanaukas, P. Quintana, L. Maldonado, R. Pomés and M.A.P. Canul, *Surf. Coat. Technol.* **92** (1997) 16.
18. J.F.S. Filho and V.F.C. Lins, *Surf. Coat. Technol.* **200** (2006) 2892.
19. G. Trejo, R.O. Borges, Y. Meas, *Plat. Surf. Finish.* (June 2002) 84.
20. G. Trejo, H. Ruiz, R.O. Borges and Y. Meas, *J. Appl. Electrochem.* **31** (2001) 685.
21. A.R. Hernandez, M.T. Ramirez and I. Gonzalez, *Anal. Chim. Acta* **278** (1993) 321.
22. A. Rojas and I. Gonzalez, *Anal. Chim. Acta* **187** (1986) 279.
23. T.V. Venkatesha, J. Balachandra, S.M. Mayanna and R.P. Dambal, *Plat. Surf. Finish.* (June 1987) 77.
24. F. Galvani and I.A. Carlos, *Met. Finish.* (February 1997) 70.
25. L. Bonou, M. Eyraud, R. Denoyel and Y. Massiani, *Electrochim. Acta* **47** (2002) 4139.
26. F. Lallemand, D. Comte, L. Ricq, P. Renaux, J. Pagetti, C. Dieppedale and P. Gaud, *Appl. Surf. Sci.* **225** (2004) 59.
27. H. Yan, J. Dawnes, P.J. Baden and S.J. Harris, *J. Electrochem. Soc.* **143** (1996) 1577.
28. A. Gomes and M.I.d.S. Pereira, *Electrochim. Acta* **51** (2006) 1342.
29. B. Reents, W. Plieth, V.A. Macagno and G.I. Lacconi, *J. Electroanal. Chem.* **453** (1998) 121.
30. Q. Qu, L. LI, W. Bai, C. Yan and C.N. Cao, *Corros. Sci.* **47** (2005) 2832.
31. N. Boshkov, *Surf. Coat. Technol.* **172** (2003) 217.
32. M. Geary and C.B. Breslin, *Corros. Sci.* **39** (1997) 1341.
33. J.B. Bajatc, V.B.M. Stankovic, M.D. Masimovic, D.M. Drazic and S. Zee, *Electrochim. Acta* **47** (2002) 4101.
34. X.G. Zhang, *Corrosion and Electrochemistry of Zinc* (Plenum Press, New-York and London, 1996), pp. 171.
35. J.B. Bajat and V.B.M. Stankovic, *Prog. Org. Coat.* **49** (2004) 183.
36. M. Gravilla, J.P. Millet, H. Mazille, D. Marchandise and J.M. Cuntz, *Surf. Coat. Technol.* **123** (2000) 164.
37. A.S. Kumar, C.S.R. Pandian, J. Ayyapparaju and G.N.K.R. Bapu, *Bull. Electrochem.* **17** (2001) 379.
38. H. Park and J.A. Szpunar, *Corros. Sci.* **40** (1998) 525.
39. K. Saber, C.C. Koch and P.S. Fedkiw, *Mater. Sci. Eng. A* **341** (2003) 174.